

Modelling spatially distributed soil losses and sediment yield in the upper Grande River Basin - Brazil

Pedro Velloso Gomes Batista, Marx Leandro Naves Silva, Bárbara Pereira Christofaro Silva, Nilton Curi, Inácio Thomaz Bueno, Fausto Weimar Acérbi Júnior, Jessica Davies, John Quinton

Angaben zur Veröffentlichung / Publication details:

Batista, Pedro Velloso Gomes, Marx Leandro Naves Silva, Bárbara Pereira Christofaro Silva, Nilton Curi, Inácio Thomaz Bueno, Fausto Weimar Acérbi Júnior, Jessica Davies, and John Quinton. 2017. "Modelling spatially distributed soil losses and sediment yield in the upper Grande River Basin - Brazil." CATENA 157: 139-50. <https://doi.org/10.1016/j.catena.2017.05.025>.

Modelling spatially distributed soil losses and sediment yield in the upper Grande River Basin - Brazil

Pedro Velloso Gomes Batista^{a,*}, Marx Leandro Naves Silva^a, Bárbara Pereira Christofaro Silva^a, Nilton Curi^a, Inácio Thomaz Bueno^b, Fausto Weimar Acérbi Júnior^b, Jessica Davies^c, John Quinton^c

^a Soil Science Department, Federal University of Lavras, Lavras, Minas Gerais, Brazil

^b Forest Engineering Department, Federal University of Lavras, Lavras, Minas Gerais, Brazil

^c Lancaster Environmental Center, Lancaster University, Lancaster, United Kingdom

A B S T R A C T

Water erosion negatively affects soil fertility, soil structure, and water availability to plants. Moreover, off-site erosion effects contribute to the sedimentation and eutrophication of water courses. The Grande River is one of the main tributaries of the Paraná River, and an important source of hydroelectric power in Brazil. The Upper Grande River Basin covers an area of 15,705 km², mostly occupied by rangelands. Shallow and little permeable Cambisols are the predominant soil class in the basin, which, combined with the intensive and highly concentrated summer rainfall, characterize an erosion-prone scenario. The aim of this study was to model the soil losses and the sediment yield in the Upper Grande River Basin. It also sought to quantify the sediment delivery to the two main hydroelectric power plant reservoirs in the basin: Camargos/Itutinga and Funil. Geographical Information Systems (GIS) were used to apply the Revised Universal Soil Loss Equation (RUSLE) and the Sediment Delivery Distributed model (SEDD) in the study area. The models were calibrated using sediment transport data obtained from a river gauging station located in a subwatershed. RUSLE predictions estimated that the average soil losses in the Upper Grande River Basin were of 22.35 t ha⁻¹ yr⁻¹, and that bare soils, eucalypt and agriculture suffered the highest erosion rates among the identified land use classes. The average specific sediment yield in the basin was of 1.93 t ha⁻¹ yr⁻¹. According to the model calibration, the specific sediment yield predictions showed an error of 0.01 t ha⁻¹ yr⁻¹, or 0.6%. Agriculture and eucalypt forests, which compose approximately 10% of the study area, contribute to more than 40% of the sediment yield in the basin. The model predictions estimated that 1.45 million t yr⁻¹ of sediments are delivered to the Camargos/Itutinga power plant reservoir, whereas the Funil power plant reservoir receives a sediment input of 1.68 million t yr⁻¹. Although model calibration yielded small errors in relation to the observed sediment measurements, the relative lack of available data has impaired a more thorough validation of the employed models. Nevertheless, the results indicate that the RUSLE/SEDD approach may be useful for analyzing sediment transport in Brazilian watersheds, where limited input data is available.

1. Introduction

Water erosion degrades soil structure, lowers soil organic matter and nutrient contents, thus reducing cultivable soil depth and depleting soil fertility (Dotterweich, 2013; Morgan, 2005). Erosion also decreases water absorption, which lowers soil moisture and water availability to plants (Pimentel, 2006). On-site soil erosion affects not only biomass, food and fiber production, but also diminishes farm income since it lowers cropland yields and increases the necessity of fertilizer applications (Poesen, 2011; Renschler and Harbor, 2002).

Off-site erosion impacts are also of great concern, especially sedimentation and eutrophication of water courses (Hu et al., 2009; Ouyang et al., 2010; Wu et al., 2012). As upland eroded sediments reach the stream network, river capacity reduces, and flood risk increases (Morgan, 2005). Sedimentation can also reduce the capacity of reservoirs, decreasing water storage and shortening the lifespan of hydroelectric power plants (Verstraeten et al., 2003).

Since direct erosion measurements are costly and time consuming, the development of soil erosion prediction models has received much attention from soil scientists. Early empirical erosion models were

* Corresponding author.

E-mail address: pbatista.ufla@gmail.com (P.V.G. Batista).

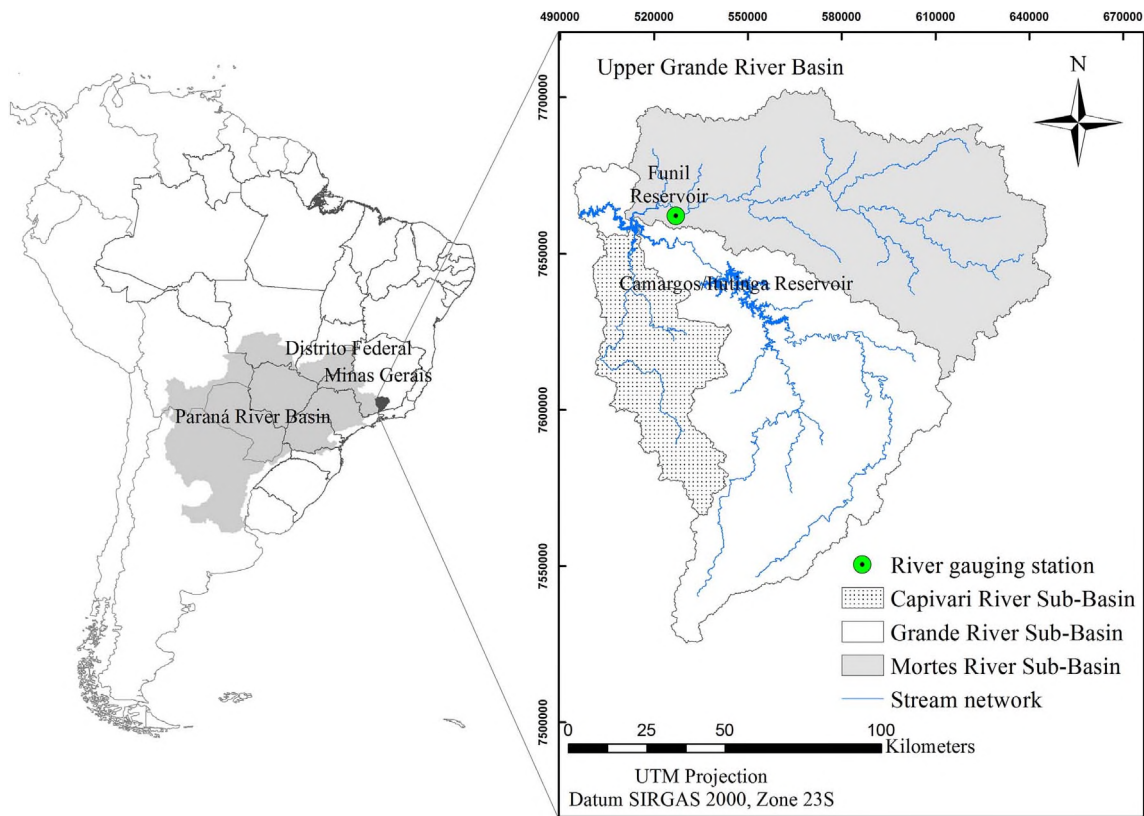


Fig. 1. Location of the Upper Grande River Basin.

developed in the USA during the 1940's and culminated with the Universal Soil Loss Equation (USLE) (Wischmeier and Smith, 1978) and its revised version (RUSLE) (Renard et al., 1997). USLE and RUSLE have been widely used, as their simple approach is useful where limited input data is available (Merritt et al., 2003; Renschler and Harbor, 2002). Although more sophisticated, process-based models are now accessible, RUSLE is still commonly employed, particularly at larger scales, through Geographic Information Systems (GIS) (Panagos et al., 2015b; Xiaoying et al., 2015; Xu et al., 2013). The combination of erosion prediction models with GIS has proved to be a powerful tool for evaluating soil losses at catchment scale, enabling the assessment of erosion rates in a distributed manner (Aksoy and Kavvas, 2005).

However, RUSLE only estimates gross erosion, providing no information on sediment delivery to water courses. Since only a fraction of upland eroded sediments reaches the catchment outlet, a sediment delivery ratio (SDR) is used to express the rate of gross erosion that eventually contributes to a river basin sediment yield (Walling, 1994). Sediment transport rates and patterns depend on many factors, such as catchment area, location of sediment sources, topographic characteristics, landscape connectivity, land use and soil texture (Vanmaercke et al., 2011; Walling, 1994). Therefore, a spatially distributed analysis of sediment production at watershed scale is critical in order to properly forecast off-site erosion impacts and to plan conservation strategies (Fernandez et al., 2003).

The Sediment Delivery Distributed (SEDD) model (Ferro and Minacapilli, 1995; Ferro and Porto, 2000) provides a semi-empirical and spatially distributed calculation of SDR. It is based on particle travel time from a given location to the nearest stream channel, following the hydraulic path of the overland flow. Ferro and Porto (2000) have suggested that during a long-period analysis, all sediments that reach the stream network are eventually discharged through the basin outlet. Therefore, the sediment delivery process could be simplified by neglecting channel deposition. The combination of RUSLE annual gross erosion predictions with SEDD by GIS processing provides

an estimation of river basin sediment yield and a spatial identification of sediment sources. Such methodology has been applied in micro-catchments in Spain (Taguas et al., 2011) and Italy (Stefano and Ferro, 2007), as well as in large river basins in Turkey (Tanyaş et al., 2015) and China (Yang et al., 2012). To the authors' knowledge, however, the SEDD model has not yet been tested under tropical conditions, such as in Brazilian watersheds.

The State of Minas Gerais, Brazil, is strategically important to water resources in Brazil and South America. The state holds the springs of Grande, Parnaíba and São Francisco rivers. The first two are the main tributaries of the Paraná River, the second longest river in South America and the main source of hydroelectric power in the country. The Upper Grande River Basin is particularly relevant regarding hydroelectric power generation, since it supplies water to two important power plants: Camargos/Itutinga and Funil, which combined have a 280 MW generation capacity.

The Upper Grande River Basin received some of earliest settlements during the colonization of the State of Minas Gerais, thus suffering environmental impacts from mining and agriculture since the late 17th century. Reports of accelerated erosion and gully formation on the northern portion of the basin can be tracked to the 19th century (Burton, 1869). More recently, studies indicate a high erosion propensity within the Upper Grande River basin due to the erodibility of the soils and the absence of agricultural conservation practices (Beskow et al., 2009; Gomide et al., 2011). However, the relative lack of river gauging stations in the region hampers direct measurements of sediment concentration in the water, which highlights the importance of erosion and sediment delivery prediction models. Given the large size of Brazilian river basins and the coarse available data, erosion models must be able to provide useful information from a restricted database.

Hence, the aim of this study was to apply the RUSLE and SEDD models, using GIS, to predict the soil losses, sediment delivery rates, and sediment yield within the Upper Grande River basin, making it possible to identify the main sediment sources in the basin; and also, to

estimate the sediment budget that annually reaches the main reservoirs of hydroelectric power plants in the study area.

2. Material and methods

2.1. Study area

The Upper Grande River Basin covers an area of 15,705 km². It stretches from the Grande River spring, in the Mantiqueira mountain range, to the Mortes River mouth, at the Funil hydroelectric power plant reservoir (Fig. 1). On the left bank of the Grande River, about 2 km upstream from the Mortes River mouth, the Capivari River flows into the reservoir. Therefore, three main subwatersheds are: the Mortes River sub-basin, to the north; the Grande River sub-basin, in the central and southern regions; and the Capivari River sub-basin, to the west. The reservoir of the Camargos/Itutinga power plant is also located at the Grande River, approximately 30 km upstream from the Funil reservoir (Fig. 1). The first has an approximate 800 hm³ water storage capacity, whilst the latter stores ca. 260 hm³.

According to the Köppen climatic classification, the prevailing climate type in the study area is Cwb – humid subtropical with dry winter and temperate summer, with an average annual precipitation of 1567 mm (Alvares et al., 2013; Hijmans et al., 2005). Granit-gneiss from the crystalline basement and pelitic rocks are the prevailing geological components, followed by quartzite rocks from the ridge formations (CPRM, 2003). Haplic Cambisols and Red Yellow Latosols are the predominant soil classes, spreading through 44% and 31% of the study area, respectively (FEAM, 2010). Haplic Cambisols are shallow, not much permeable and often graveled, usually associated to hilly, mountainous slopes; Red Yellow Latosols are severely weathered, deep, very permeable soils, usually found in the flatter, gentle slopes along the landscape (Menezes et al., 2009). Rangeland is the primary land use, frequently degraded by overgrazing and water erosion (Table 1). Elevations range from about 800 m, near the basin outlet, to 2600 m, at the Mantiqueira mountain ridges (Table 2).

2.2. RUSLE modeling

RUSLE estimates average annual soil losses by a direct equation in which five empirical factors are used to describe the processes affecting erosion (Renard et al., 1997):

$$A = R * K * LS * C * P \quad (1)$$

where: A is soil loss per unit area (t ha⁻¹ yr⁻¹); R is the rainfall and runoff erosivity factor (MJ mm ha⁻¹ h⁻¹ yr⁻¹); K is soil erodibility factor (t ha h ha⁻¹ MJ⁻¹ mm⁻¹); LS is the topographic factor, representing slope length and steepness (dimensionless); C is cover management factor (dimensionless), and P is support practice factor (dimensionless).

Table 1
Land use in the Upper Grande River Basin and main sub-watersheds.

Land use	Upper Grande River Basin	Sub-basin		
		Capivari	Grande	Mortes
	Area (%)			
Agriculture	5.5	9.0	5.4	4.6
Bare soil	0.2	0.4	0.1	0.1
Eucalypt	4.7	3.2	4.7	5.2
Forest	25.6	25.0	29.6	21.6
Rangeland	59.1	45.9	56.2	66.2
Rupestrian vegetation ^a	3.5	15.9	2.2	1.0
Urban area	0.6	0.2	0.3	1.1
Water	0.8	0.4	1.5	0.2

^a Grassland formations with predominance of the herbaceous and sub-shrubby layers, usually associated to rocky outcrops and litholic soils (Andrade, 2013).

Table 2
Morphological attributes of the main sub-basins within the Upper Grande River Basin.

Attribute		Sub-basin		
		Capivari	Grande	Mortes
Altitude (m)	Min	807	784	807
	Max	1768	2649	1412
	Mean	1051	1102	1035
	Std	114	207	85
Slope (°)	Min	0	0	0
	Max	62	71	68
	Mean	9	10	9
	Std	5	7	5

For spatial modeling purposes, ArcGIS 10.1 (ESRI, 2011) was used to compose grid layers of each RUSLE factor, enabling the application of map algebra tools to the georeferenced grid cell values. The output maps are presented in a 30 m resolution, which was standardized according to the cell size of the input rasters (mainly the DEM, and the land use map). The methodologies for composing these layers, as well as the necessary input data (Fig. 2), are described as follows.

2.2.1. Rainfall-runoff erosivity factor (R)

The EI₃₀ index is used to represent raindrop impact and surface runoff capacity to generate soil losses when all other erosion parameters are held constant (Renard et al., 1997). The index is computed for individual rainstorms as the product of a storm's total kinetic energy (E) (MJ ha⁻¹ mm⁻¹) times the storm's maximum 30 minute intensity (mm h⁻¹) (Foster et al., 1981). The R factor for RUSLE is calculated as the sum of EI₃₀ values over a specific time period (Renard et al., 1997; Wischmeier and Smith, 1978).

Since EI₃₀ computation requires rather detailed, not always available data, equations linking rainfall coefficients – such as the Fournier index – to EI₃₀ values have been developed for different locations (Lazzari et al., 2015; Mello et al., 2007). In this study, we have used the equation proposed by Aquino et al. (2014) for Lavras, a city northwest of the Upper Grande River basin:

$$EI_{30} = 85.672 * Rc^{0.6557} \quad (2)$$

$$Rc = \frac{p^2}{P} \quad (3)$$

where: Rc is Fournier's rainfall coefficient (mm); p is average monthly rainfall (mm) and P is average annual rainfall (mm).

In order to spatially represent the R factor, average monthly and annual rainfall layers were obtained from the WorldClim database (Fig. 2a) (Hijmans et al., 2005). WorldClim provides climate grids interpolated from various weather stations, using data comprised between the years of 1950 to 2000 (Hijmans et al., 2005). The rainfall grids were clipped within the study area and resampled to a 30 m grid cell resolution. Eq. (2) was applied to the monthly rainfall layers, and the sum of resulting grids was calculated to represent average annual EI₃₀, i.e. the R factor for the Upper Grande River basin.

2.2.2. Soil erodibility factor (K)

Conceptually, soil erodibility expresses the propensity of a soil to suffer particle detachment by raindrop impact and surface runoff (Renard et al., 1997). It is therefore influenced by a number of soil properties, such as hydraulic conductivity, surface roughness, soil texture and mineralogy. Quantitatively, the K factor is the rate of soil loss per erosion index unit as measured in a unit plot (22.13 m long, 9% slope, plowed downslope and kept continuously fallow) (Wischmeier and Smith, 1978).

In this study, K factor values were taken from the available scientific literature (Table 3). All of the chosen factors were calibrated for Brazilian soils and priority was given to the factors obtained from plot

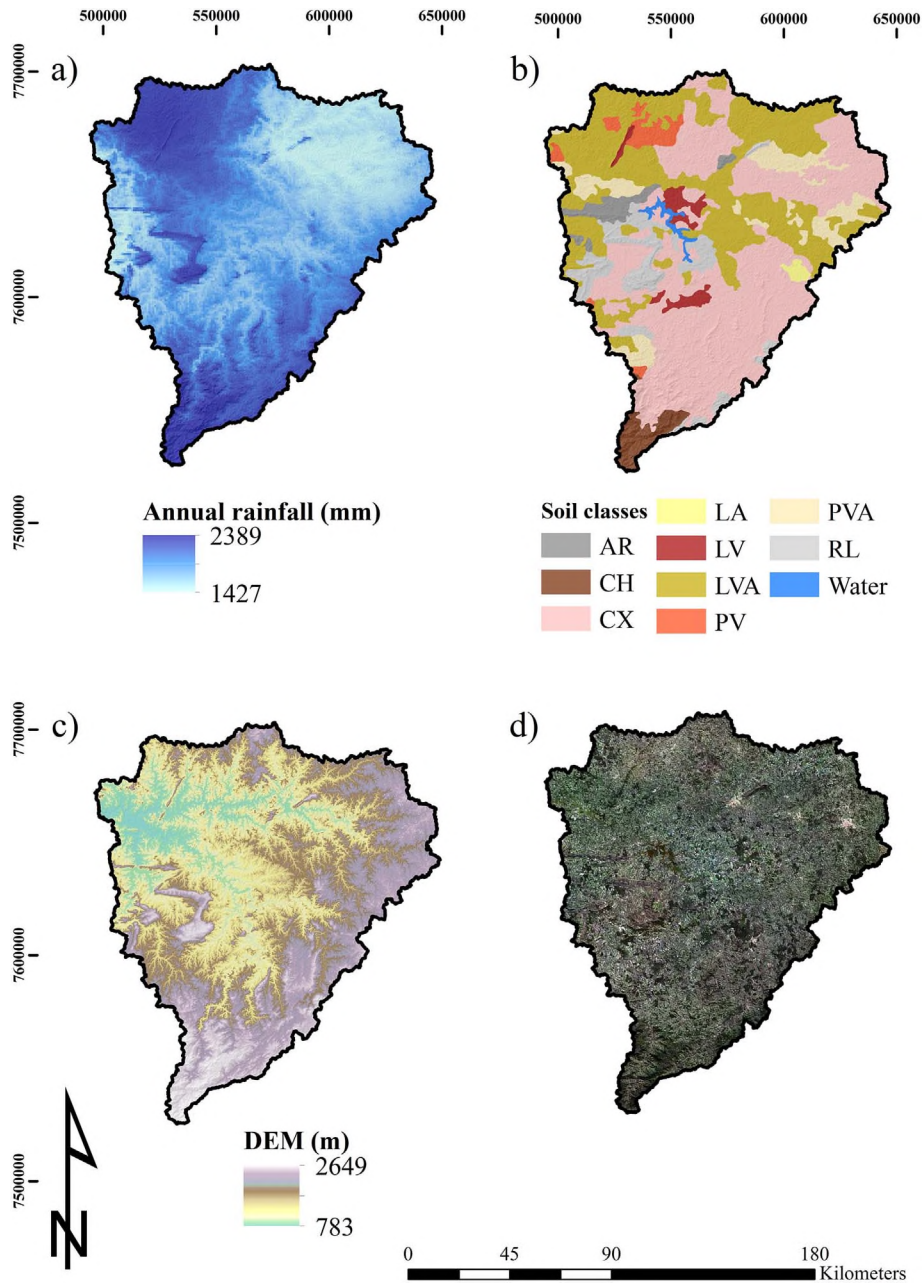


Fig. 2. GIS input data for RUSLE modeling in the Upper Grande River Basin: (a) annual rainfall grid (Hijmans et al., 2005); (b) soil map (FEAM, 2010); (c) Digital Elevation Model; (d) Landsat imagery.

Soil map legend: AR: rock outcrop; CH: Humic Cambisol; CX: Haplic Cambisol; LA: Yellow Latosol; LV: Red Latosol; LVA: Red Yellow Latosol; PV: Red Argisol; PVA: Red Yellow Argisol; RL: Litholic Neosol. (For interpretation of the references to colour in this figure legend, the reader is referred to the web version of this article.)

based, natural rainfall experiments.

The soil map of the State of Minas Gerais (scale 1:650,000) was used to assign K factor values according to the soil classes existing in the Upper Grande River Basin (Fig. 2b) (FEAM, 2010). The soil map shapefile was converted into a 30 m resolution raster, where grid cell values represented soil erodibility.

2.2.3. Topographic factor (*LS*)

The topographic factor in USLE and RUSLE expresses the influence of slope length (*L*) and slope angle (*S*) on soil erosion. These parameters, however, are not easily determined at catchment scale, under non-uniform slopes and complex geomorphologic situations (Garcia Rodriguez and Gimenez Suarez, 2012).

In an attempt to improve USLE/RUSLE application at natural landscape scenarios, Mitasova et al. (1996) proposed an equation for

estimating the *LS* factor through GIS, following the concept of upslope contributing area introduced by Moore and Burch (1986) as a replacement for the slope length parameter:

$$LS = (m + 1) * \left(\frac{U}{22.13} \right)^m * \left(\frac{\sin \theta}{0.0896} \right)^n \quad (4)$$

where: *U* (m) is the upslope contributing area per contour width (or cell resolution); θ is slope angle; *m* and *n* are empirical parameters that range from 0.4–0.6 and 1.0–1.4, respectively, depending on the prevailing type of erosion (sheet or rill).

The use of upslope contributing area for the computation of the *LS* factor provides a spatial identification of flow patterns, which yields higher erosion predictions as flow convergence increases (Mitasova et al., 2013). However, RUSLE is not applied where concentrated flow exists. Hence, if no limit is imposed for parameter *U* from Eq. (4),

Table 3
Soil classes and respective soil erodibility (K factor) values.

Soil class	Area (%)	K factor (t ha h ha ⁻¹ MJ ⁻¹ mm ⁻¹)	Source
AR	5.0	0.0000	–
CH	2.6	0.0105	Bertol et al. (2002)
CX	44.4	0.0355	Silva et al. (2009)
LA	0.5	0.0090	Silva et al. (2000)
LV	2.1	0.0032	Silva et al. (2009)
LVA	30.8	0.0100	Silva et al. (2000)
PV	2.5	0.0320	Marques et al. (1997)
PVA	7.0	0.0106	Eduardo et al. (2013)
RL	4.4	0.0567	Castro et al. (2011)

Legend: AR: rock outcrop; CH: Humic Cambisol; CX: Haplic Cambisol; LA: Yellow Latosol; LV: Red Latosol; LVA: Red Yellow Latosol; PV: Red Argisol; PVA: Red Yellow Argisol; RL: Litholic Neosol.

extreme erosion rates may be predicted by the model. Fernandez et al. (2003), Fu et al. (2006), and Yang et al. (2012) have suggested a limit of 120 m, following the recommendation of McCool et al. (1997), which states that flow usually concentrates in less than 400 ft (121.92 m).

In this study, the LS factor was calculated according to Eq. (4), using ArcGIS 10.1 map algebra tools (ESRI, 2011). Assuming the prevalence of sheet erosion, given the fact that grasslands and forests are the main land uses in the basin, parameters m and n where set as 0.4 and 1.0, respectively. Slope angle (θ) was derived from a 30 m resolution DEM obtained from SRTM (Shuttle Radar Topography Mission) imagery (Fig. 2c). Parameter U was determined by further DEM processing: TauDEM 5.1.2 toolset (Tarboton, 2014) for ArcGIS 10.1 (ESRI, 2011) was used to calculate upslope contributing area based on a D^∞ flow direction algorithm (Tarboton, 1997).

By setting a limit of 120 m for parameter U (considering a 30 m DEM resolution, this translates to an upslope area 3600 m²), we noticed that many hillslopes were being identified as flow concentration areas, when, in reality, rill and interrill erosion were still the dominant processes. Hence, we increased such limit to 360 m, which yielded a more reasonable spatial description of flow concentration. Such value is based on field and remote sensing observations from the study area, and therefore, it may be very site specific. However, it should be highlighted that tropical, weathered soils, usually display high hydraulic conductivity and high infiltration rates. Hence, it is not unexpected that large contributing areas are necessary for the water flow to concentrate in channels, hollows or ephemeral gullies in such conditions.

2.2.4. Cover-management factor (C)

The C factor expresses the weighted ratio of soil losses on a given land use situation in relation to the ones measured in a unit plot (Renard et al., 1997). Therefore, it reflects not only land cover, but also crop type, tillage practices and other management conditions (Panagos et al., 2015a). C factor values range from 0 to 1.0 with low values being densely vegetated landscapes, such as forested areas, and higher values relating to bare soils.

For erosion modeling at catchment scale, C factor values from the scientific literature can be assigned to uniform land use classes (Panagos et al., 2015a). In this study, land cover maps were produced using 30 m resolution Landsat 8 Surface Reflectance images, dated from 2013 (Fig. 2d). An object-oriented classification was performed using a fuzzy rule-based approach, through eCognition Developer software (Trimble, 2010). Finally, C factor values were appointed to the identified land use classes (Table 4). Urban areas were excluded from the analysis, mostly due to the lack of an adequate C factor value to represent such land use category, and also due to the negligible area occupied by villages and towns in the basin (0.6%). The C factor value estimated for rangelands was also applied for rupestrian vegetation, given that the factor has not yet been calibrated for this specific land use category.

Table 4
Land uses and respective C factor values.

Land use	C factor	Source
Agriculture	0.156	De Maria and Lombardi Neto (1997)
Bare soil	1.000	Wischmeier and Smith (1978)
Eucalypt	0.121	Silva et al. (2016)
Forest	0.015	Silva et al. (2016)
Rangeland	0.025	Dedecek et al. (1986)
Ruspestrian vegetation	0.025	Dedecek et al. (1986)

2.2.5. Support practice factor (P)

Field observation of the Upper Grande River Basin showed no consistent soil conservation practices. Although some contour tillage/seeding practices can be found on more technified agricultural areas, these are rare and difficult to identify, given the large study area and the coarse available satellite imagery. Therefore, a single P factor value of 1.0 was assigned to all the study area.

2.3. SEDD modeling

In the SEDD model, SDR_i expresses the probability that eroded particles, on a given upland location, will reach the nearest stream channel (Ferro and Minacapilli, 1995). SDR_i values range from 0 to 1.0, which quantify the percentage of gross erosion that is delivered to the stream network, and eventually, to the catchment outlet, since the model neglects channel deposition. This study used SEDD equations in a grid based methodology proposed by Jain and Kothyari (2000):

$$SDR_i = \exp(-\beta t_i) \quad (5)$$

where: SDR_i is the soil delivery ratio of a grid cell i ; β is a catchment specific parameter (h^{-1}) and t_i is the overland flow travel time (h) from a grid cell i to the nearest stream channel along the flow path.

Overland flow travel time from a grid cell to the nearest stream channel along the flow path was computed as:

$$t_i = \frac{l_i}{v_i} \quad (6)$$

where: l_i is the flow length from cell i to the nearest stream channel (m) and v_i is the flow velocity for cell i ($m s^{-1}$).

The flow length parameter for Eq. (6) was calculated using the D8 Distance to Streams function of the TauDEM 5.1.2 (Tarboton, 2014) toolset for ArcGIS 10.1 (ESRI, 2011). By inputting a DEM derived flow path grid and stream network grid, the algorithm computes the horizontal distance to streams, moving downslope according to the flow path.

Flow velocity was calculated observing Jain and Kothyari (2000), which incorporated the US Soil Conservation Service equation for overland and shallow channel flow (SCS, 1975) to the SEDD model:

$$v_i = a_i S_i^{0.5} \quad (7)$$

where: a_i is a surface roughness coefficient for cell i ($m s^{-1}$) and S_i is the slope for cell i ($m m^{-1}$).

As the a_i coefficient for Eq. (7) is dependent on land cover, values were assigned according to the land use map (Table 5).

Specific sediment yield (SSY_i) ($t ha^{-1} yr^{-1}$) quantifies the area specific amount of eroded sediment that reaches the catchment outlet. It can be determined as (Jain and Kothyari, 2000):

$$SSY_i = SDR_i A_i \quad (8)$$

where: SSY_i is the specific sediment yield for a grid cell i ; SDR_i is the soil delivery ratio for a grid cell i and A_i is the annual soil loss computed by RUSLE for a grid cell i .

The total sediment yield (SY) ($t yr^{-1}$) of a river basin is estimated by multiplying the mean modeled SSY_i values by catchment area. In places where gauging stations provide measurements of river water

Table 5
Values of a_i .
Adapted from Haan et al. (1994)

Land use	a (m s^{-1})
Agriculture	2.62
Bare soil	3.08
Eucalypt	1.56
Forest	0.76
Rangeland	0.76
Ruspestrian vegetation	0.76

sediment concentration, both SSY and SY can be directly estimated (Walling, 1994). These measurements are used to calibrate and evaluate model forecasts (Jetten and Maneta, 2011). In this study, the β parameter from Eq. (5) was calibrated using SY data from the Mortes River. The methodologies for calculating SY and for calibrating the SEDD model are discussed in the following sections.

2.3.1. Measured sediment yield

The Brazilian National Water Agency (ANA) supplies data from a number of river gauging stations. Although daily discharge data is commonly assessed at these stations, total solids in the water are rarely measured. Even so, the latter measurements are sparse and often discontinuous. In this study, the Funil hydroelectric power plant provided the only recent and continuous information on the total solids in the water within the Upper Grande river Basin. The data was collected at a gauging station in the Mortes River, at the Ibituruna municipality, about 20 km upstream from the Funil reservoir. Suspended and bottom sediment concentration, as well as water discharge, were observed on a monthly basis from March 2008 to April 2012. This data was used to plot a discharge curve, which related total sediments in the water (mg L^{-1}) to river discharge ($\text{m}^3 \text{s}^{-1}$) (Fig. 3). Daily discharge values for the same gauging station, obtained from the ANA database, were applied to the discharge curve in order to better represent the variation of discharge and sediment transport during a longer period of time. Data comprised from January 2002 to May 2010 was applied to discharge curve. Average annual SY was then calculated, as well as the SSY for the gauging station catchment area.

2.3.2. Model calibration

According to Ferro and Porto (2000), the catchment specific coefficient β for Eq. (5) lumps the spatial effects of roughness and runoff along the hydraulic flow path, also varying at a temporal scale. Although the authors suggested some deductive approaches for determining β at event scale, the coefficient has been often calibrated by adjusting the parameter to best fit the observed SY values (Fernandez

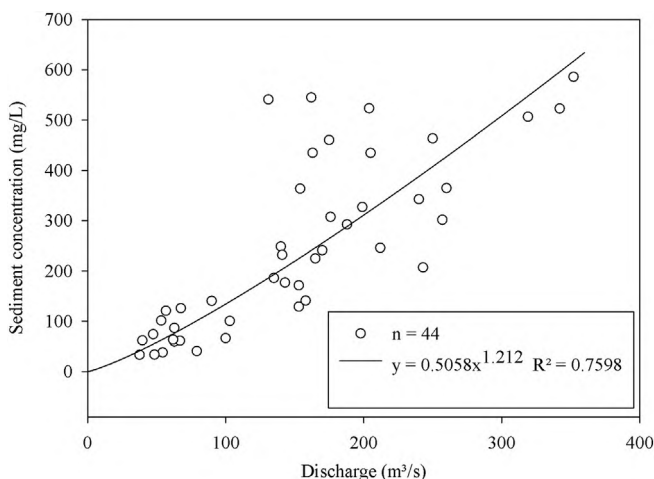


Fig. 3. Discharge curve for the Mortes River at the Ibituruna gauging station.

et al., 2003; Fu et al., 2006; Lin et al., 2016; Yang et al., 2012).

In this study, β was calibrated using measured sediment data from the Ibituruna gauging station. The catchment area of the station site was derived from the DEM, using ArcGIS 10.1 (ESRI, 2011) hydrology tools. As the station was close to the Mortes River mouth, catchment area (6040 km^2) was similar to the area of Mortes River sub-basin (6609 km^2). The best adjustment for β was found by comparing the SSY values obtained from the discharge curve to the mean SSY_i values estimated by the model within the gauging station catchment area (Eq. (8)). The best-fit value of β (which yielded the lowest error in relation to the observed SSY) was then applied to the SEDD equations in the whole Upper Grande River Basin. Although the assumption that β is constant throughout the basin may be questionable (Porto and Walling, 2015), a series of sediment yield measurements within sub-catchments, which are not available at present, would be necessary to establish independent β values.

2.3.3. Trap efficiency

Trap efficiency (TE) is used to express the proportion of incoming sediments that is deposited in a reservoir (Verstraeten and Poesen, 2000). Although sediment concentrations measurements from upstream and downstream a reservoir should supply an accurate estimation of TE, such measurements are not commonly available in many developing countries. An alternative approach is provided by empirical equations based on a capacity-inflow ratio (C/I) (e.g. Brune, 1953). In this study we used Brune's (1953) curve to estimate the TE of the Funil and Camargos/Itutinga reservoirs. Annual water inflow was determined based on historical discharge data upstream from the reservoirs. The calculated C/I ratios for the reservoirs were applied to Brune's median TE curve, assuming a mixture of coarse and fine-grained inflowing sediments. The input data and the equations used for calculating TE are summarized in Table 6.

3. Results and discussion

3.1. RUSLE model

Annual rainfall erosivity in the Upper Grande River Basin ranged from 5193 to $7027 \text{ MJ mm ha}^{-1} \text{ h}^{-1} \text{ yr}^{-1}$, with an average of $5546 \text{ MJ mm ha}^{-1} \text{ h}^{-1} \text{ yr}^{-1}$. Such values are in agreement with the ones determined for the south of the State of Minas Gerais by Aquino et al. (2012), which ranged from 5145 to $7776 \text{ MJ mm ha}^{-1} \text{ h}^{-1} \text{ yr}^{-1}$. Spatially, greater erosivity was associated with higher elevation. The Mantiqueira mountain range, in the southern region of the study area, presented the highest values of rainfall erosivity (Fig. 4a).

Red Yellow Latosols compose most of the northern section of the Upper Grande River Basin, whereas Haplic Cambisols are widespread on the southern and eastern portions. This soil class distribution meant lower K factor values within the Mortes River sub-basin when compared to the Grande River sub-basin. Most of the Litholic Neosols in the study area are mapped within the Capivari River sub-basin. These soils are very shallow and coarsely textured, which contributes to increase the erosion propensity in the subwatershed (Fig. 4b).

The calculated LS factor varied from 0, in the very flat valleys where slope angle was null, to 43.74, at the steep hillslopes and flow

Table 6
Input data and equations for calculating reservoir trap efficiency.

Reservoir	C (hm^3)	I (hm^3)	C/I	TE equation*
Camargos/Itutinga	260	10,218	0.025	$97 - \left(1.275 \left \ln \left(\frac{C}{I} \right) \right ^{2.47} \right)$
Funil	800	3437	0.233	

Legend: C: reservoir storage capacity; I: annual water inflow; C/I: capacity-inflow ratio; TE: trap efficiency.

* Source: Verstraeten and Poesen (2000).

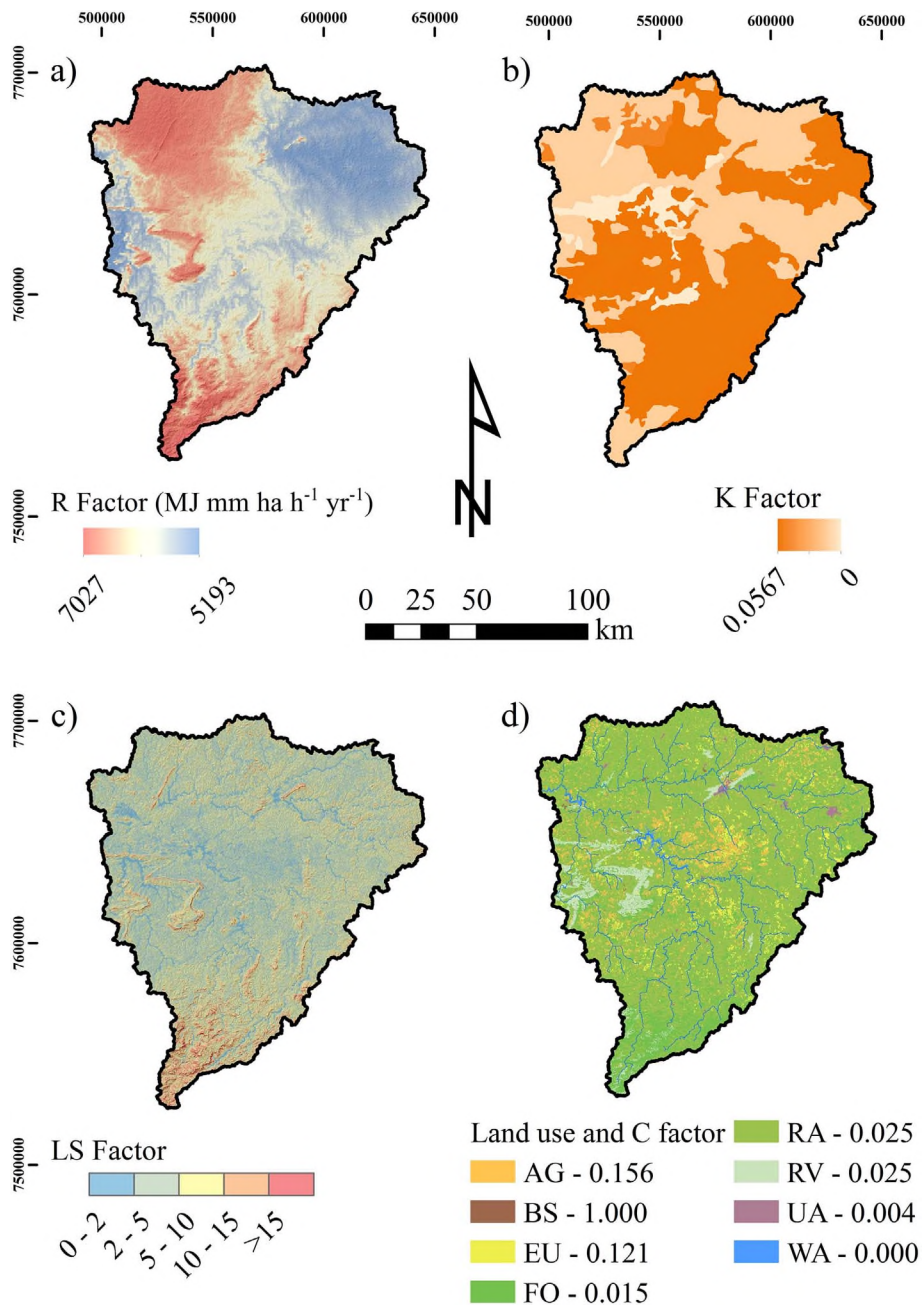


Fig. 4. Layers of the RUSLE factors for the Upper Grande River Basin: (a) R factor, (b) K factor, (c) LS factor and (d) C factor. Land use map legend: AG: agriculture; BS: bare soil; EU: eucalypt; FO: forest; RA: rangeland; RV: rupestrian vegetation; UA: urban area; WA: water.

convergence areas (Fig. 4c). The average value was of 4.99.

RUSLE predictions of average annual soil losses for the Upper Grande River Basin were of $22.35 \text{ t ha}^{-1} \text{ yr}^{-1}$ (Fig. 5). Rangelands, the main land use in the study area, presented average soil losses of $16.63 \text{ t ha}^{-1} \text{ yr}^{-1}$. Many pastures found in the basin are degraded, and therefore, may experience greater erosion than well-managed rangelands. Also, during the beginning of the rainy season, pastures are usually sparsely vegetated as a result of overgrazing and the lack of rainfall during the winter. Therefore, the single C factor value appointed to such land use might not represent the spatial and temporal variability of the parameter, which associates uncertainty to the model predictions.

Although the same C factor value was assigned to rangeland and rupestrian vegetation, RUSLE estimations, in the latter case, showcased $33.25 \text{ t ha}^{-1} \text{ yr}^{-1}$ average soil losses. This stems from the fact that rupestrian vegetation is strongly associated with ridge formations and

Litholic Neosols, the most erodible soil class in the basin.

Gross erosion predictions for forest areas of $16.21 \text{ t ha}^{-1} \text{ yr}^{-1}$ were higher than the usual USLE/RUSLE estimations for such land use in Brazilian watersheds (Avanzi et al., 2013; Silva et al., 2016). As remaining native forests in the Upper Grande River Basin are mostly located on drainage lines and very steep slopes, which are improper for agriculture or grazing, the model predicted a great propensity to soil erosion. The mean LS factor value for forests was 33% and 94% higher than the ones for rangeland and agriculture, respectively. It is pertinent to point out that although soil losses on cultivated lands have a strong relation to slope length and slope angle, the same cannot be confirmed for dense, naturally vegetated areas, where hydraulic conductivity is high and extremely variable (Govers, 2011). Therefore, RUSLE predictions of erosion rates for forests may be overestimated in this study.

The average soil losses for eucalypt and agriculture were of 65.93 and $57.29 \text{ t ha}^{-1} \text{ yr}^{-1}$, respectively, in spite of the greater C factor

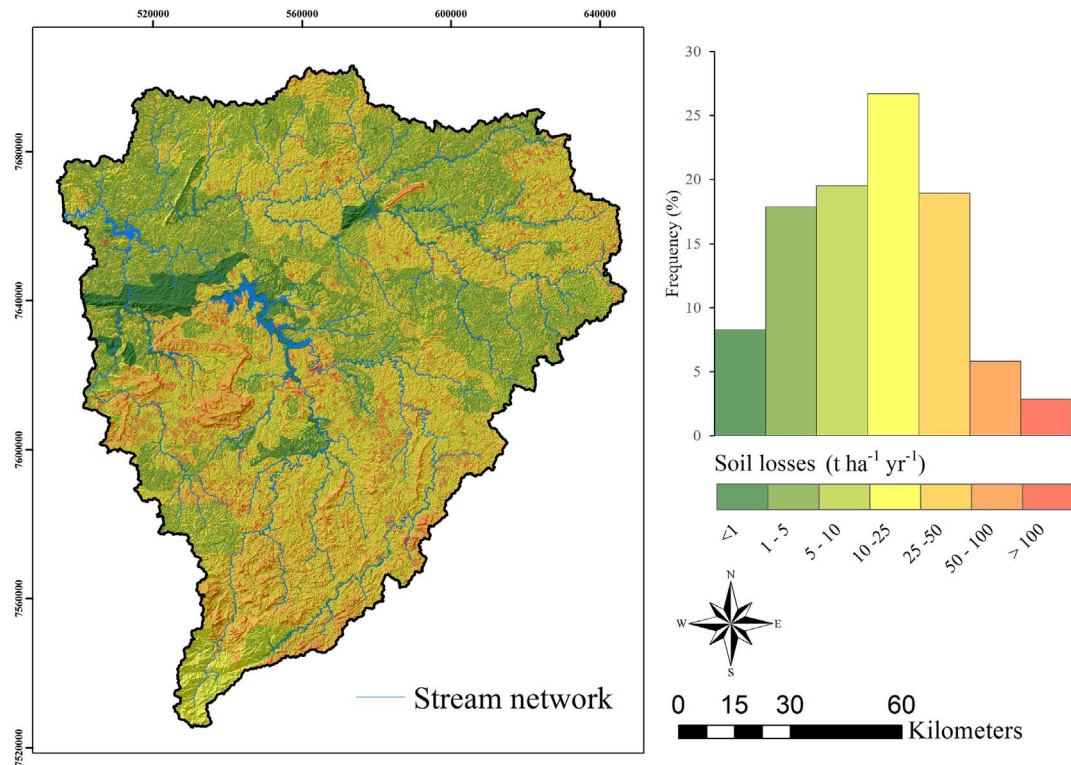


Fig. 5. Average annual soil losses in the Upper Grande River Basin.

assigned to croplands. In the Upper Grande River Basin, agricultural areas are mainly located where less erodible soils occur; that means 59% of the croplands were found on Latosols, whereas eucalypt was mainly associated with Haplic Cambisols. Also, agriculture tends to be established on smooth landscapes, more suited to mechanization. Mean values of the LS factor for croplands were 17% lower than those of eucalypt forests. As stated by [Silva et al. \(2014\)](#), eucalypt plantations in Brazil are often situated in vulnerable ecosystems, on previously degraded areas with steep slopes and highly erodible soils.

The highest erosion predictions were associated with bare soils, where average soil losses were of $604.58 \text{ t ha}^{-1} \text{ yr}^{-1}$. In the study area, bare soils consisted of fallow and degraded soils, as well as strip mines and unpaved roads.

Regarding the gross erosion rates on the three main subwatersheds of the study area, RUSLE predicted soil losses of 26.97, 26.18 and $16.81 \text{ t ha}^{-1} \text{ yr}^{-1}$ for the Capivari River, the Grande River and the Mortes River sub-basins, respectively. Land use distribution and rainfall erosivity were found to be rather similar among the subwatersheds. Therefore, the contrast of erosion intensity can be explained by the variation of topography and, primarily, of soil erodibility, as mentioned before.

3.2. SEDD model

3.2.1. Measured data and model calibration

According to the discharge curve for the Ibituruna gauging station, the average annual SSY in the Mortes River Basin was of $1.59 \text{ t ha}^{-1} \text{ yr}^{-1}$, with a 2.9% coefficient of variation (CV). Correlation analysis between monthly rainfall erosivity and SSY showed a coefficient of determination of 73%. However, monthly SSY did not increase directly with erosivity, given that eroded sediments do not reach the catchment outlet immediately, and are remobilized several times before being discharged. During the end of the rainy season, in April, although rainfall erosivity declines, SSY is still significant. Such behavior is possibly explained by the fact that previously eroded particles continue to be transported by the stream network (Fig. 6).

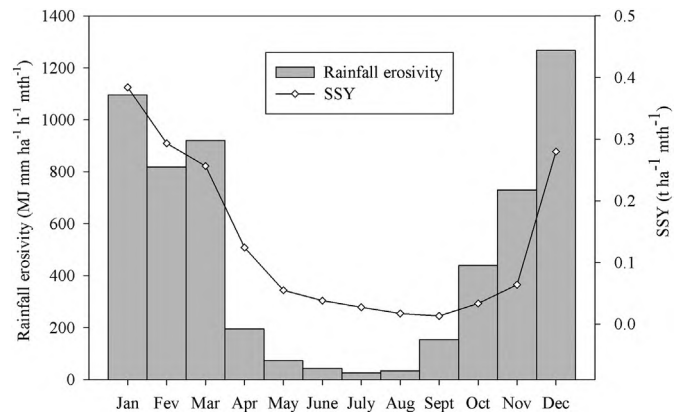


Fig. 6. Average monthly specific sediment yield and rainfall erosivity for the Mortes River sub-basin, upstream from the Ibituruna gauging station.

The calibration of the β coefficient for the SEDD equation indicated that the model was sensitive to the parameter. Average modeled SSY_i for the Mortes River sub-basin varied 58% as β ranged from 1.0 to 4.0 h^{-1} . By setting the β parameter to 3.0 h^{-1} , SEDD predictions yielded a mean SSY_i value of $1.58 \text{ t ha}^{-1} \text{ yr}^{-1}$, which resulted in an error of $0.01 \text{ t ha}^{-1} \text{ yr}^{-1}$, or 0.6%.

It is important to highlight that the β parameter may be a source of great uncertainty in the SEDD model. The parameter highly increases the user's degree of freedom, and the model is able to accommodate a wide range of results during calibration of β . Uncertainty and sensitivity analysis should be employed to verify the model's prediction capacity, as performed by [Stefano and Ferro \(2007\)](#). However, the lack of proper validation data in the study area hampered such investigation. Nevertheless, the calibrated β value in this study was similar to the ones reported by [Yang et al. \(2012\)](#). According to the authors, the best SEDD model results for two river basins, with 4500 and 7140 km^2 , were obtained with β values of 3.2 and 4.6 h^{-1} , respectively. According to [Lin et al. \(2016\)](#), the calibrated β value for a watershed with 486 km^2 in

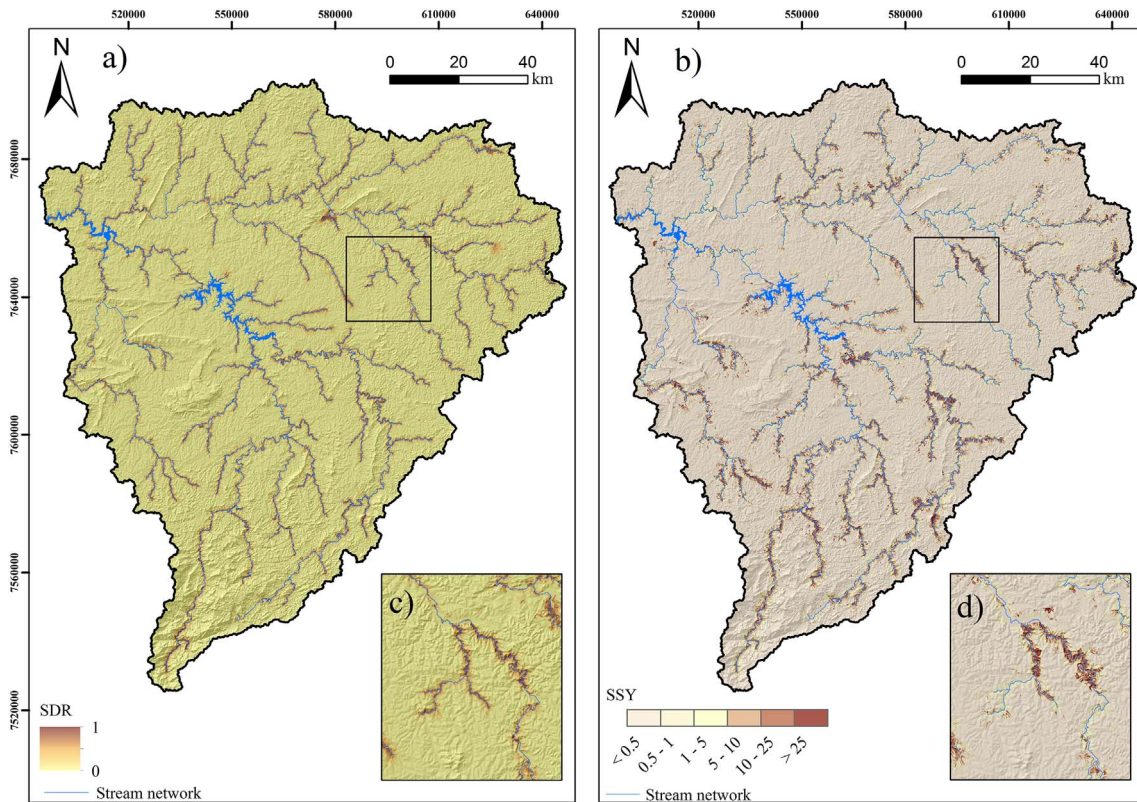


Fig. 7. (a) (b) Sediment delivery rate and (c) (d) specific sediment yield ($\text{t ha}^{-1} \text{yr}^{-1}$) in the Upper Grande River Basin.

China was of 0.304 h^{-1} ; whereas Fu et al. (2006) reported that a β of 1.0 h^{-1} yielded the best predictions of SSY for a 327 km^2 watershed. Hence, although β theoretically lumps the effects of roughness and runoff along the hydraulic path, the coefficient seems to have some empirical relation with catchment area. According to Eq. (5), SDR_i will decrease as β increases. As the highest reported β values relate to larger watersheds, and SDR overall tends to decrease with catchment area (Walling, 1994), it is to be expected that calibrated β values will generally increase with watershed size. However, the relation between β and catchment area may not be straight-forward and attempts to estimate β from catchment characteristics have been unsuccessful (Porto and Walling, 2015).

3.2.2. Sediment delivery ratio, specific sediment yield and total sediment yield

Once the β coefficient was calibrated for the Mortes River sub-basin, the best-fit value of 3.0 was applied to the Upper Grande River Basin, which resulted in the SDR_i layer displayed in Fig. 7a.

The mean value of SDR_i for the study area was of 0.07. The spatial distribution of SDR_i indicates that the sediment sources closer to the stream channels have higher probability of delivering eroded particles to the water courses. However predictable this might look, flow velocity, which depends on slope gradient and surface roughness, is used in the SEDD model as a proxy for overland flow transport capacity. Therefore, wherever flow velocity is high, eroded particles have a greater possibility of being transported to the stream network as opposed to being deposited along hillslopes. As surface roughness was determined according to land use, predictions of SDR_i were influenced by such parameter (Table 7).

Correlation analysis between surface roughness (parameter a of Eq. (7)) and mean SDR_i values for the land use classes showed a coefficient of determination of 97%. These results differ from the ones of Fernandez et al. (2003) and Fu et al. (2006), in which SDR_i did not exhibit a clear relation with land use.

Since parameter a is constant for a specific land use, the CV of SDR_i

Table 7

SDR_i values according to the different land uses in the Upper Grande River Basin.

Land use	SDR_i Mean	Coefficient of variation (%)
Agriculture	0.13	60.12
Bare soil	0.16	72.78
Eucalypt	0.09	49.93
Forest	0.06	36.00
Rangeland	0.06	37.86
Rupestrian vegetation	0.03	26.32

reflects the spatial variability of the distance to streams and slope gradient. Land uses with very specific geographical distribution, such as the rupestrian vegetation, had a lower variability of SDR_i . On the other hand, the high CV for bare soils demonstrates that such land use does not have an obvious geographical pattern concerning slope and proximity to water courses (Table 6).

The average SSY_i in the Upper Grande River was of $1.93 \text{ t ha}^{-1} \text{yr}^{-1}$ (Fig. 7b). The distance to streams did not influence SSY_i values as much as it influenced SDR_i . The zoom-in data frames in Fig. 7c and d demonstrate how SSY_i varies within a close distance to the stream channel. Such behavior is expected since SSY_i depends on the gross erosion rates. This means that, even if a given sediment source is closely located to the stream network, and transport capacity of the overland flow is high, SSY_i will not be expressive if particle detachment is low.

According to the SEDD model predictions, bare soils had the highest average SSY_i among the land uses of the study area (Table 8). These results are connected to the extremely high erosion rates predicted by RULSE in such land use class. Also, the average values of SDR_i for bare soils indicated a greater propensity of sediment delivery to streams in comparison to other land uses. Bare soils comprise only 0.16% of the study area. Nonetheless, the model estimated that almost 9% of the total SY in the Upper Grande River basin originates from fallow or

Table 8
Mean SSY_i , SY and percentage of SY according to the land use classes in the Upper Grande River Basin.

Land use	SSY_i	SY	
	$t\ ha^{-1}\ yr^{-1}$	$t\ yr^{-1}$	%
Agriculture	8.82	767,370	25.4
Bare soil	110.94	268,831	8.9
Eucalypt	7.21	534,885	17.7
Forest	0.91	368,066	12.2
Rangeland	1.12	1,040,978	34.4
Rupestrian vegetation	0.77	42,670	1.4

degraded soils, strip mines and unpaved roads (Table 8).

Agriculture produced the second highest SSY_i values. Although croplands comprise only 5.5% of the study area, such land use generated 25% of the total SY in the basin. Eucalypt forests also showed expressive SSY_i values, which were only lower than the ones for bare soils and agriculture (Table 8). Rangeland and forests which, combined, occupy 85% of the Upper Grande River Basin account for only 46% of the total SY. Therefore, according to the model predictions, sediment production in the study area is highly influenced by intensive land use.

Since the SEDD model neglects channel deposition, it is assumed that all sediments that reach the stream network will be discharged through the river basin outlet. In the Grande River sub-basin, upstream from the Camargos/Itutinga reservoir, average values of SSY_i were of $2.32\ t\ ha^{-1}\ yr^{-1}$. Therefore 1.45 million $t\ yr^{-1}$ of sediments are delivered into the reservoir, considering a catchment area of 624,300 ha. These results differ from the ones presented by Beskow et al. (2009). According to these authors, SSY upstream from the reservoir was of $0.81\ t\ ha^{-1}\ yr^{-1}$. Although these estimations were based on river gauging station data, they may not be representative of current conditions, since the information was comprised between 1996 and 2003. Also, in the same study, river sediment concentration was only evaluated 5 times per year, and as such sediment yields may be underestimated. However, given the lack of recent sediment measurements upstream from the Camargos/Itutinga reservoir, the SEDD model could not be tested; hence, the SSY_i results from this study should be analyzed with caution.

TE for the Camargos/Itutinga reservoir is estimated at 94%. Therefore, we assumed that a sediment load of 1.36 million $t\ yr^{-1}$ is deposited in the reservoir, whereas 0.09 million $t\ yr^{-1}$ of sediments are transported downstream from the dam.

The SEDD model predictions indicated that the primary source of sediments in the Funil reservoir is the Mortes River, which delivers 1.04 million $t\ yr^{-1}$ of sediments into the reservoir. This result is supported by recent bathymetric surveys, which indicate the Mortes River delta is the main sedimentation zone in the Funil reservoir (Soares, 2015). Navigation is already hampered in the shallow delta waters, given the amount of deposited sediments.

The average SSY_i values in the Capivari River sub-basin was of $2.34\ t\ ha^{-1}\ yr^{-1}$. The river drains an area of 207,800 ha, which transports a total of 486,960 $t\ yr^{-1}$ of sediments into the Funil reservoir. Considering the drainage area downstream from the Itutinga/Camargos reservoir, as well as the sediments that transverse the Camargos/Itutinga dam, the Grande River transports 146,804 $t\ yr^{-1}$ of sediments. Therefore, the modeling results indicate that the average sediment delivery to the Funil reservoir is of 1.68 million $t\ yr^{-1}$. TE for the reservoir is estimated at 65%, and hence, 1.09 million t of sediments are annually deposited.

Recent bathymetric surveys have indicated that the annual loss of storage capacity in the Funil reservoir is of $2.8\ hm^3$ (Soares, 2015). Since bulk density of the bottom sediments in the reservoir could not be evaluated, a comparison between the model predictions and the

sediment deposition could not be properly achieved. Nevertheless, considering these values, it seems reasonable to state that RUSLE and SEDD underestimated the amount of sediments that reach the Funil reservoir annually. Model underestimation could be attributable to the following: RUSLE soil loss estimations do not represent the erosion dynamics in permanent gullies, river bank erosion, and landslides, which may be a significant source of sediments in river basins (Verstraeten et al., 2003); the temporal effects of over-grazing are not captured by RUSLE and the C coefficient, and the extreme precipitation events may not be well represented. Mispredictions may also originate due the assumption that the stream network provides no sources or sinks regarding catchment sediment yield. This assumption stems from the conception that the fluvial system and hillslope sediment yield are in a long-term quasi-equilibrium condition. This condition may not be applicable in situations where land use has been altered: in such cases, the fluvial system can be an important regulator of sediment yield, which may reflect the recent historical dynamics of erosion and sediment delivery in a river basin (Walling, 1994).

It is important to point out that although reservoir bathymetric surveys supply the most accurate estimations of river basins SY, such evaluations are not free from errors (de Vente et al., 2013; Verstraeten et al., 2003). In the case of the Funil reservoir, the recent work of Soares (2015) is based on very densely sampled bathymetric surveys. Previous surveys in the area, however, were not as detailed, and the reservoir storage capacity might not have been precisely estimated.

4. Conclusions

In the Upper Grande River Basin, bare soils, eucalypt forests and agriculture presented the highest soil losses among the identified land cover classes, according to the RUSLE predictions. Therefore, soil conservation planning should focus on these land uses, and eucalypt forests should receive special attention. The model depicted that, in the study area, eucalypts are located on steep hillslopes with erosion-prone soils, and experience severe soil losses.

The results from the SEDD model indicated that, within the identified land uses classes, rangelands are the main source of sediments in Upper Grande River Basin. However, that stems from the fact that pastures comprise most of the study area. Bare soils, agriculture and eucalypt presented the highest area-specific sediment yield values. Such land uses generate a great amount of sediment within relatively small areas. Hence, in order to reduce the off-site erosion impacts in the basin, soil management support practices on croplands and eucalypt forests should be widely encouraged. Moreover, the identification and rehabilitation of degraded bare soils may further decrease the sediment yield in the basin.

Also according to the SEDD model results, sedimentation in the Funil reservoir is mostly linked to sediments transported by the Mortes River. These results are corroborated by field observation and recent bathymetric surveys. The Camargos/Itutinga reservoir receives a similar annual sediment input as does the Funil reservoir. However, the latter may experience greater sedimentation rates due to its lower storage capacity. Given the relevance of the Upper Grande River Basin in generating hydroelectric power, the monitoring of sediment fluxes into the basin's main reservoirs should be intensified.

It is important to point out that the results provided by this study are an initial estimation of the erosion and sediment delivery dynamics in the Upper Grande River Basin. Field data must be gathered in order to verify the quantity and the sources of sediments that reach the water courses. Although the modeling results from this study have been successfully calibrated, much uncertainty can be associated to the predictions. A model may accurately predict the sediment yield from a river basin without correctly identifying the spatial source, especially when calibration from observed data is employed. In the case of the SEDD model, the basin-specific coefficient β strongly increases the user's degree of freedom, and also, the uncertainty of the predictions.

The validation of erosion prediction models is inherently problematic, given the spatial and temporal variability of the phenomenon. Nevertheless, validation efforts should be increased, especially when models are applied in situations for which they were not developed. A more robust validation dataset must be gathered in order to properly evaluate the performance of the RULSE/SEDD modeling under tropical conditions. Initial results, however, indicate that the approach may be useful for analyzing sediment transport in Brazilian watersheds, where limited input data is available.

Acknowledgments

This research was funded in part by Coordination of Superior Level Staff Improvement – CAPES, the National Counsel of Technological and Scientific Development – CNPq (Process n° 471522/2012-0 and 305010/2013-1), and Minas Gerais State Research Foundation – FAPEMIG (Process n° CAG-PPM-00422-13). The authors are thankful for the comments from Dr Gert Verstraeten and the anonymous reviewers who read this manuscript and helped to improve the quality of the paper.

References

- Aksoy, H., Kavvas, M.L., 2005. A review of hillslope and watershed scale erosion and sediment transport models. *Catena* 64, 247–271. <http://dx.doi.org/10.1016/j.catena.2005.08.008>.
- Alvares, C.A., Stape, J.L., Sentelhas, P.C., de Moraes Gonçalves, J.L., Sparovek, G., 2013. Köppen's climate classification map for Brazil. *Meteorol. Z.* 22, 711–728. <http://dx.doi.org/10.1127/0941-2948/2013/0507>.
- Andrade, E.A., 2013. Composição florística e estrutura da vegetação de campos rupestres sobre quartzito do “Complexo Serra da Boicaina”, MG. (PhD Thesis) Universidade Federal de Lavras, Lavras.
- Aquino, R.F., Silva, M.L.N., Freitas, D.A.F., Curi, N., Mello, C.R., Avanzi, J.C., 2012. Spatial variability of the rainfall erosivity in southern region of Minas Gerais state, Brazil. *Cienc. Agrotecnol.* 36, 533–542.
- Aquino, F., Silva, M.L.N., Freitas, D.A.F., Curi, N., Mello, C.R., Avanzi, J.C., 2014. Erosividade das chuvas e tempo de recorrência para Lavras, Minas Gerais. *Ceres* 61, 09–16.
- Avanzi, J.C., Silva, M.L.N., Curi, N., Norton, L.D., Beskow, S., Martins, S.G., 2013. Spatial distribution of water erosion risks in a watershed with eucalyptus and atlantic forest. *Cienc. Agrotecnol.* 37, 427–434.
- Bertol, I., Schick, J., Batistela, O., Leite, D., Amaral, A.J., 2002. Erodibilidade de um Cambissolo Húmico aluminóico léptico, determinada sob chuva natural entre 1989 e 1998 em Lages (SC). *R. Bras. Ci. Solo* 36, 465–471.
- Beskow, S., Mello, C.R., Norton, L.D., Curi, N., Viola, M.R., Avanzi, J.C., 2009. Soil erosion prediction in the Grande River Basin, Brazil using distributed modeling. *Catena* 79, 49–59. <http://dx.doi.org/10.1016/j.catena.2009.05.010>.
- Brune, G.M., 1953. Trap efficiency of reservoirs. *Trans. Am. Geophys. Union* 34, 407–418.
- Burton, R., 1869. *Explorations of the Highlands of Brazil*. Tinsley Brothers, London.
- Castro, W.J., Lemke-De-Castro, M.L., Lima, J.O., Oliveira, L.F.C., Rodrigues, C., Figueiredo, C.C., 2011. Erodibilidade de solos do cerrado goiano. *Revista em Agronegócios e Meio Ambiente* 4, 305–320.
- CPRM - Serviço Geológico Do Brasil, 2003. *Mapa geológico do estado de Minas Gerais*. CPRM, Brasília (Escala 1:1.000.000).
- De Maria, I.C., Lombardi Neto, F., 1997. Razão de perdas de solo e fator C para sistemas de manejo da cultura do milho. *Rev. Bras. Ci. Solo* 21, 263–270.
- De Vente, J., Poesen, J., Verstraeten, G., Govers, G., Vanmaercke, M., Van Rompaey, A., Arabkhedri, M., Boix-Fayos, C., 2013. Predicting soil erosion and sediment yield at regional scales: where do we stand? *Earth Sci. Rev.* 127, 16–29. <http://dx.doi.org/10.1016/j.earscirev.2013.08.014>.
- Dedecek, R.A., Resck, D.V.S., Freitas, E., 1986. Perdas de solo, água e nutrientes por erosão em Latossolo Vermelho-Escuro dos cerrados em diferentes cultivos sob chuva natural. *Rev. Bras. Ci. Solo* 10, 265–272.
- Dotterweich, M., 2013. The history of human-induced soil erosion: geomorphic legacies, early descriptions and research, and the development of soil conservation—a global synopsis. *Geomorphology* 201, 1–34. <http://dx.doi.org/10.1016/j.geomorph.2013.07.021>.
- Eduardo, E.N., Carvalho, D.F., Machado, R.L., Soares, P.F.C., Almeida, W.S., 2013. Erodibilidade, fatores cobertura e manejo e práticas conservacionistas em Argissolo Vermelho-Amarelo, sob condições de chuva natural. *Rev. Bras. Ci. Solo* 37, 796–803.
- ESRI - Environmental Systems Research Institute, 2011. *ArcGIS for Desktop, Version 10.1*. (Redlands.CD ROM).
- FEAM - Fundação Estadual Do Meio Ambiente, 2010. *Mapa de solos de Minas Gerais: legenda expandida*. FEAM/UFV/CETEC/UFLA, Belo Horizonte.
- Fernandez, C., Wu, J.Q., Mccool, D.K., Stockle, C.O., 2003. Estimating water erosion and sediment yield with GIS, RUSLE, and SEDD. *J. Soil Water Conserv.* 58, 128–136.
- Ferro, V., Minacapilli, M., 1995. Sediment delivery processes at basin scale. *Hydrol. Sci. J.* 40, 703–717. <http://dx.doi.org/10.1080/02626669509491460>.
- Ferro, V., Porto, P., 2000. Sediment delivery distributed (SEDD) model. *J. Hydrol. Eng.* 5, 411–422.
- Foster, G.R., McCool, D.K., Renard, K.G., 1981. Conversion of the universal soil loss equation to SI metric units. *J. Soil Water Conserv.* 31, 355–359.
- Fu, G., Chen, S., McCool, D.K., 2006. Modeling the impacts of no-till practice on soil erosion and sediment yield with RUSLE, SEDD, and ArcView GIS. *Soil Tillage Res.* 85, 38–49. <http://dx.doi.org/10.1016/j.still.2004.11.009>.
- García Rodríguez, J.L., Gimenez Suarez, M.C., 2012. Methodology for estimating the topographic factor LS of RUSLE3D and USPED using GIS. *Geomorphology* 175–176, 98–106. <http://dx.doi.org/10.1016/j.geomorph.2012.07.001>.
- Gomide, P.H.O., Silva, M.L.N., Soares, C.R.F.S., 2011. Atributos físicos, químicos e biológicos do solo em ambientes de voçorocas no município de Lavras - MG. *Rev. Bras. Ci. Solo* 35, 567–577.
- Govers, G., 2011. Misapplications and misconceptions of erosion models. In: Morgan, R.P.C., Nearing, M.A. (Eds.), *Handbook of Erosion Modeling*. Blackwell Publishing Ltd, Oxford, pp. 117–134.
- Haan, C.T., Barfield, B.J., Hayes, J.C., 1994. *Design Hidrology and Sedimentology for Small Catchments*. Academic Press, San Diego.
- Hijmans, R.J., Cameron, S.E., Parra, J.L., Jones, P.G., Jarvis, A., 2005. Very high resolution interpolated climate surfaces for global land areas. *Int. J. Climatol.* 25, 1965–1978. <http://dx.doi.org/10.1002/joc.1276>.
- Hu, B., Yang, Z., Wang, H., Sun, X., Bi, N., Li, G., 2009. Sedimentation in the Three Gorges Dam and the future trend of Changjiang (Yangtze River) sediment flux to the sea. *Hydrol. Earth Syst. Sci.* 13, 2253–2264.
- Jain, M.K., Koithyari, U.C., 2000. Estimation of soil erosion and sediment yield using GIS. *Hydrol. Sci. J.* 45, 771–786.
- Jetten, V.G., Maneta, M.P., 2011. Calibration of erosion models. In: Morgan, R.P.C., Nearing, M.A. (Eds.), *Handbook of Erosion Modeling*. Blackwell Publishing Ltd, Oxford, pp. 33–51.
- Lazzari, M., Gioia, D., Piccarreta, M., Danese, M., Lanorte, A., 2015. Sediment yield and erosion rate estimation in the mountain catchments of the Camastra artificial reservoir (Southern Italy): a comparison between different empirical methods. *Catena* 127, 323–339. <http://dx.doi.org/10.1016/j.catena.2014.11.021>.
- Lin, C., Wu, Z., Ma, R., Su, Z., 2016. Detection of sensitive soil properties related to non-point phosphorus pollution by integrated models of SEDD and PLOAD. *Ecol. Indic.* 60, 483–494. <http://dx.doi.org/10.1016/j.ecolind.2015.07.023>.
- Marques, J.J.G.S.M., Curi, N., Ferreira, M.M., Lima, J.M., Silva, M.L.N., Carolino De Sá, M.A., 1997. Adequação de métodos indiretos para a estimativa de erodibilidade de solos com horizonte B textural no Brasil. *Rev. Bras. Ci. Solo* 21, 447–456.
- McCool, D.K., Foster, G.R., Weesies, G.A., 1997. Slope-length and steepness factors. In: Enard, K.G., Foster, G.R., Weesies, G.A., Mccool, D.K., Yoder, D.C. (Eds.), *Predicting Soil Erosion by Water: A Guide to Conservation Planning With the Revised Universal Soil Loss Equation*. U.S. Department of Agriculture, Washington, pp. 101–142.
- Mello, C.R. De, Aurélio, M., Sá, C. De, Curi, N., Mello, J.M. De, 2007. Erosividade mensal e anual da chuva no Estado de Minas Gerais. *Pesq. Agrop. Brasileira* 30, 537–545.
- Menezes, M.D., Curi, N., Marques, J.J., Mello, C.R., Araújo, A.R., 2009. Levantamento pedológico e Sistema de Informações Geográficas na avaliação do uso das terras em sub-bacia hidrográfica de Minas Gerais. *Cienc. Agrotecnol.* 33, 1544–1553.
- Merritt, W.S., Letcher, R.A., Jakeman, A.J., 2003. A review of erosion and sediment transport models. *Environ. Model. Softw.* 18, 761–799. [http://dx.doi.org/10.1016/S1364-8152\(03\)00078-1](http://dx.doi.org/10.1016/S1364-8152(03)00078-1).
- Mitasova, H., Hofierka, J., Zlocha, M., Iverson, L.R., 1996. Modeling topographic potential for erosion and deposition using GIS. *Int. J. Geogr. Inf. Sci.* 10, 629–641.
- Mitasova, H., Barton, M., Hofierka, J., Harmon, R.S., 2013. GIS-based soil erosion modeling. In: Shroder, J.F. (Ed.), *Treatise on Geomorphology*. Academic Press, San Diego, pp. 228–258.
- Moore, I.D., Burch, G.J., 1986. Modeling erosion and deposition: topographic effects. *Trans. ASAE* 29, 1624–1640.
- Morgan, R.P.C., 2005. *Soil Erosion & Conservation*, third ed. Blackwell, Oxford.
- Ouyang, W., Hao, F., Skidmore, A.K., Toxopeus, A.G., 2010. Soil erosion and sediment yield and their relationships with vegetation cover in upper stream of the Yellow River. *Sci. Total Environ.* 409, 396–403. <http://dx.doi.org/10.1016/j.scitotenv.2010.10.020>.
- Panagos, P., Borrelli, P., Meusburger, K., Alewell, C., Lugato, E., Montanarella, L., 2015a. Estimating the soil erosion cover-management factor at the European scale. *Land Use Policy* 48, 38–50. <http://dx.doi.org/10.1016/j.landusepol.2015.05.021>.
- Panagos, P., Borrelli, P., Poesen, J., Ballabio, C., Lugato, E., Meusburger, K., Montanarella, L., Alewell, C., 2015b. The new assessment of soil loss by water erosion in Europe. *Environ. Sci. Pol.* 54, 438–447. <http://dx.doi.org/10.1016/j.envsci.2015.08.012>.
- Pimentel, D., 2006. Soil erosion: a food and environmental threat. *Environ. Dev. Sustain.* 8, 119–137. <http://dx.doi.org/10.1007/s10668-005-1262-8>.
- Poesen, J., 2011. Challenges in gully erosion research. *Landf. Anal.* 17, 5–9.
- Porto, P., Walling, D.E., 2015. Use of Caesium-137 measurements and long-term records of sediment load to calibrate the sediment delivery component of the SEDD model and explore scale effect: examples from Southern Italy. *J. Hydrol. Eng.* 20 (C4014005-1-C4014005-12).
- Renard, K.G., Foster, G.R., Weesies, G.A., Mccool, D.K., Yoder, D.C., 1997. *Predicting Soil Erosion by Water: A Guide to Conservation Planning With the Revised Universal Soil Loss Equation*. U.S. Department of Agriculture, Washington.
- Renschler, C.S., Harbor, J., 2002. Soil erosion assessment tools from point to regional scales—the role of geomorphologists in land management research and implementation. *Geomorphology* 47, 189–209. [http://dx.doi.org/10.1016/S0169-555X\(02\)00082-X](http://dx.doi.org/10.1016/S0169-555X(02)00082-X).
- SCS (Soil Conservation Service), 1975. *Urban hydrology for small watersheds*. Technical release n. 55. Soil Conservation Service United States Department of Agriculture, Washington DC, USA.

- Silva, M.L.N., Curi, N., Lima, J.M., Ferreira, M.M., 2000. Avaliação de métodos indiretos de determinação da erodibilidade de Latossolos Brasileiros. *Pesq. Agrop. Brasileira* 35, 1207–1220.
- Silva, A.M., Silva, M.L.N., Curi, N., Avanzi, J.C., Ferreira, M.M., 2009. Erosividade da chuva e erodibilidade de Cambissolo e Latossolo na região de Lavras, sul de Minas Gerais. *Rev. Bras. Ci. Solo* 33, 1811–1820.
- Silva, M.A., Silva, M.L.N., Curi, N., Oliveira, A.H., Avanzi, J.C., Norton, L.D., 2014. Water erosion risk prediction in eucalyptus plantations. *Ciênc. agric.* 38, 160–172.
- Silva, B.C.P., Silva, M.L.N., Batista, P.V.G., Pontes, L.M., Araújo, E.F. De, Curi, N., 2016. Soil and Water Losses in Eucalyptus Plantation and Natural Forest and Determination of the USLE Factors at a Pilot Sub-basin in Rio Grande do Sul, Brazil. 40. pp. 432–442.
- Soares, W.S., 2015. Taxa de assoreamento no reservatório da Usina Hidrelétrica do Funil - MG. (MS Thesis) Universidade Federal de Lavras, Lavras.
- Stefano, C. Di, Ferro, V., 2007. Evaluation of the SEDD model for predicting sediment yield at the Sicilian experimental SPA2 basin. *Earth Surf. Process. Landf.* 32, 1094–1109. <http://dx.doi.org/10.1002/esp>.
- Taguas, E.V., Moral, C., Ayuso, J.L., Pérez, R., Gómez, J.a., 2011. Modeling the spatial distribution of water erosion within a Spanish olive orchard microcatchment using the SEDD model. *Geomorphology* 133, 47–56. <http://dx.doi.org/10.1016/j.geomorph.2011.06.018>.
- Tanyaş, H., Kolat, Ç., Süzen, M.L., 2015. A new approach to estimate cover-management factor of RUSLE and validation of RUSLE model in the watershed of Kartalkaya Dam. *J. Hydrol.* 528, 584–598. <http://dx.doi.org/10.1016/j.jhydrol.2015.06.048>.
- Tarboton, D.G., 1997. A new method for the determination of flow directions and upslope areas in grid elevation models. *Water Resour. Res.* 33, 309–319.
- Tarboton, D.G., 2014. TauDEM 5.1.2: terrain analysis using digital elevation models. Available in: <http://hydrology.usu.edu/taudem/taudem5/downloads.html> (Access on: August 15, 2014).
- Trimble, 2010. eCognition® Developer 8.64.0 Reference Book. (Available at: <http://www.definiens.com/>. Access on may 11, 2015).
- Vanmaercke, M., Poesen, J., Verstraeten, G., de Vente, J., Ocakoglu, F., 2011. Sediment yield in Europe: spatial patterns and scale dependency. *Geomorphology* 130, 142–161. <http://dx.doi.org/10.1016/j.geomorph.2011.03.010>.
- Verstraeten, G., Poesen, J., 2000. Estimating trap efficiency of small reservoir and ponds. *Prog. Phys. Geogr.* 24, 219–251.
- Verstraeten, G., Poesen, J., de Vente, J., Koninckx, X., 2003. Sediment yield variability in Spain: a quantitative and semiquantitative analysis using reservoir sedimentation rates. *Geomorphology* 50, 327–348. [http://dx.doi.org/10.1016/S0169-555X\(02\)00220-9](http://dx.doi.org/10.1016/S0169-555X(02)00220-9).
- Walling, D.E., 1994. Measuring sediment yield from river basins. In: Lal, R. (Ed.), *Soil Erosion Research Methods*. Soil and Water Conservation Society, Washington, pp. 39–82.
- Wischmeier, W.H., Smith, D.D., 1978. *Predicting Rainfall Erosion Losses: A Guide to Conservation Planning*. USDA, Washington.
- Wu, C.-H., Chen, C.-N., Tsai, C.-H., Tsai, C.-T., 2012. Estimating sediment deposition volume in a reservoir using the physiographic soil erosion-deposition model. *Int. J. Sediment Res.* 27, 362–377. [http://dx.doi.org/10.1016/S1001-6279\(12\)60041-9](http://dx.doi.org/10.1016/S1001-6279(12)60041-9).
- Xiaoying, L., Shi, Q., Yuan, H., Yuehong, C., Pengfei, D., 2015. Predictive modeling in sediment transportation across multiple spatial scales in the Jialing River Basin of China. *Int. J. Sediment Res.* <http://dx.doi.org/10.1016/j.ijsrc.2015.03.013>.
- Xu, L., Xu, X., Meng, X., 2013. Risk assessment of soil erosion in different rainfall scenarios by RUSLE model coupled with information diffusion model: a case study of Bohai Rim, China. *Catena* 100, 74–82. <http://dx.doi.org/10.1016/j.catena.2012.08.012>.
- Yang, M., Li, X., Hu, Y., He, X., 2012. Assessing effects of landscape pattern on sediment yield using sediment delivery distributed model and a landscape indicator. *Ecol. Indic.* 22, 38–52. <http://dx.doi.org/10.1016/j.ecolind.2011.08.023>.